Cu Valency Change Induced by O Doping in YBCO

W. M. Temmerman,[1] H. Winter,[2] Z. Szotek,[1] and A. Svane[3]

[1]*Daresbury Laboratory, Daresbury, Warrington WA4 4AD, Cheshire, United Kingdom*
[2]*INFP, Forschungszentrum Karlsruhe GmbH, Postfach 3640, D-76021 Karlsruhe, Germany*
[3]*Institute of Physics and Astronomy, University of Aarhus, DK-8000 Aarhus C, Denmark*
(Received 6 November 2000)

An *ab initio* local spin density study of $YBa_2Cu_3O_6$, $YBa_2Cu_3O_{6.5}$, and $YBa_2Cu_3O_7$ is presented. The method includes self-interaction corrections for the Cu d states, which enables a description of various valency configurations of both planar and chain Cu atoms. For $YBa_2Cu_3O_6$ the antiferromagnetic and insulating state is described with planar (chain) Cu occurring in a divalent (trivalent) state. The evolution in the CuO_2 plane from insulating to metallic behavior upon oxygenation is accomplished by the delocalization of the majority Cu $d_{x^2-y^2}$−O2 p_x−O3 p_y band.

An understanding of the changes, upon doping, in the electronic structure of the high T_c superconductors might contribute to the elucidation of the richness in their physical properties which include an apparent competition between an antiferromagnetic phase and a superconducting state [1]. Reliable materials specific calculations which allow for oxygen variation would be extremely useful in this context. However, standard band theory calculations fail to describe the antiferromagnetic insulating state of the parent compounds of the high T_c materials [2]: The local spin density (LSD) approximation gives an inadequate description of the electron-electron interactions for these strongly correlated systems. More specifically, from a susceptibility analysis of the LSD wave functions [3], it became clear that the LSD wave functions of the Cu d electrons and, in particular, those of t_{2g} symmetry were not sufficiently localized on the Cu sites. The subsequent application to La_2CuO_4 of the self-interaction correction (SIC) [4] to LSD led to the correct ground state [5]. The corresponding electronic structure was such that for the Cu sites in CuO_2 planes, the five Cu d electrons of the majority spin channel, and the three $d_{t_{2g}}$ and one d_{3z^2-1} electrons in the minority spin channel, were moving in a self-interaction corrected potential. The gap was formed between the bonding and antibonding states of O p_x and p_y with the minority Cu $d_{x^2-y^2}$ state, for which no self-interaction correction was applied.

The electronic properties of the superconducting materials, such as $YBa_2Cu_3O_7$, seem to be well described by the LSD. In particular, the Fermi surface is in good agreement with experiment. Controversial, however, is the absence of bilayer splitting [6] and the nature of the saddle point, giving rise to the Van Hove singularity in the density of states, stemming from the Cu $d_{x^2-y^2}$ and the O2 p_x, O3 p_y orbitals lying in the CuO_2 planes. With the possibility of an important role of the Van Hove singularity for the high T_c superconductivity [7], in this Letter we study with the SIC-LSD approach the electronic structure of $YBa_2Cu_3O_6$, $YBa_2Cu_3O_{6.5}$, and $YBa_2Cu_3O_7$ (YBCO for short). While the application of the SIC maintains the LSD band picture

description of the electronic properties, it also allows one to make contact with an ionic description. The SIC-LSD scheme allows "localized" electrons to move in a different (self-interaction corrected) potential, compared to the fast-moving normal conduction electrons, thus reflecting the full relaxation of the atomic ion to the stationarity of the localized electron. In particular, the SIC moves the spectral weight of the localized electrons far below the Fermi level, which contributes to the gap formation [8].

In what follows, total energy calculations are reported with various configurations, Cu^+, Cu^{2+}, and Cu^{3+}, for both the planar (Cu_{pl}) and chain (Cu_{ch}) Cu atoms. Specifically, the Cu^+, Cu^{2+}, and Cu^{3+} configurations correspond to calculations where the self-interaction correction is implemented, respectively, for all ten, for nine, or for eight Cu d states. In Table I all studied Cu d configurations are summarized and explained. The remaining electrons, namely, one in the case of Cu^+, two for Cu^{2+}, and three for Cu^{3+}, are described by the LSD potentials; i.e., they will form Bloch states, for which self-interaction is negligible, and their chemical and angular momentum characters are determined by the self-consistent LSD theory. In other words, the manifold of d states is in part described by SIC-LSD potentials and in part by LSD potentials. Since the foundation of the SIC-LSD scheme is a total energy functional, the specification of particular Cu ionic configurations corresponds to exploring different parts of the allowed configuration space, and, in particular, the energy

TABLE I. Different Cu configurations (conf.) defining the total number and symmetries of the Cu d orbitals to be self-interaction corrected (SIC orbitals). The remaining Cu d states are described with LSD band theory.

| | SIC Orbitals | |
Cu conf.	Cu majority d channel	Cu minority d channel
d^{10}	5	5
d^9	5	4 $[3(t_{2g}) + 1(3z^2 - 1)]$
d^{9*}	5	4 $[3(t_{2g}) + 1(x^2 - y^2)]$
d^8	4 $[3(t_{2g}) + 1(3z^2 - 1)]$	4 $[3(t_{2g}) + 1(3z^2 - 1)]$
d^{8*}	4 $[3(t_{2g}) + 1(x^2 - y^2)]$	4 $[3(t_{2g}) + 1(x^2 - y^2)]$

comparison of different configurations is possible, as has been recently demonstrated in the rare earths [9].

The SIC-LSD [10] has been implemented within the linear-muffin-tin-orbital atomic-sphere-approximation (LMTO-ASA) method in the basis of the screened muffin-tin orbitals [11]. To improve on the standard ASA the nonspherically symmetric Madelung terms have been included both in the potential construction and in the total energy expression. Furthermore, empty spheres have been introduced in the Y plane and in the plane of the CuO chain. The partial waves used are Ba $6s$, $5p$, $5d$, $4f$; Y $5s$, $4p$, $4d$, $4f$; Cu $4s$, $4p$, $3d$; O $2s$, $2p$, $3d$ and empty sphere $1s$, $2p$. The Ba $4f$, Y $4f$, O $3d$, and empty sphere $2p$ partial waves have been described as intermediate waves [11]. The structural parameters have been taken from [12], [13], and [14] for $YBa_2Cu_3O_6$, $YBa_2Cu_3O_{6.5}$, and $YBa_2Cu_3O_7$, respectively. The screened structure constants have been constructed with a cluster of about 100 atoms around each of the positions in the unit cell. The same cluster has been used for the real space representation of the SIC-LSD potentials.

The total energy differences for various Cu configurations and three different YBCO compounds are presented in Table II. In these calculations the Cu's are antiferromagnetically ordered in both directions in the tetragonal plane giving rise to a doubling of the unit cell. For $YBa_2Cu_3O_6$ the total energy is minimized in the configuration of divalent (d^9) and magnetic Cu_{pl} and trivalent (d^{8*}) and nonmagnetic Cu_{ch}, which corresponds to the experimental high-temperature magnetic structure [15]. A spin magnetic moment of $0.60\mu_B$ for Cu_{pl} is calculated for this ground state configuration which compares well with the observed value of $0.47\mu_B$. Magnetic order of the Cu_{ch} is realized in the configuration d^{9*}, but this is energetically unfavorable by 1.2 eV; here the Cu_{ch} atom attains a magnetic moment of $0.35\mu_B$. Thus, the experimental high-temperature magnetic structure with antiferromagnetically ordered Cu_{pl} and no magnetic order on the Cu_{ch} is correctly described. To investigate more complex magnetic structures such as possible antiferromagnetic

order along the c direction, which is the observed low-temperature magnetic structure [15], would entail another doubling of the unit cell which is beyond the present state of the art.

A striking feature of the results in Table II is that the Cu valence energy differences for different chain configurations are fairly independent of the valency configuration in the plane and, likewise, the Cu valence energy differences for different plane configurations are more or less independent of the valency configuration in the chain. Specifically, for $YBa_2Cu_3O_6$, the energy associated with the Cu_{pl} d^9 to d^8 fluctuation is approximately 0.5 eV (actually varies between 0.35 and 0.6 eV), when Cu_{ch} is in either the d^8, d^{8*}, d^9, d^{9*}, or the d^{10} configuration. For Cu_{ch} the fluctuations away from d^{8*} involve energies in excess of 1.2 eV and, in particular, the monovalent d^{10} configuration is 3.9 eV away from the ground state. Therefore our ground state solution does not obey a standard ionic picture of divalent Cu_{pl} and monovalent Cu_{ch} and instead the ground state of $YBa_2Cu_3O_6$ is quite stable with respect to divalent Cu in the CuO_2 plane and a trivalent valency for the Cu_{ch}.

Figure 1a shows the density of states of $YBa_2Cu_3O_6$ in the ionic configuration of Cu_{ch}^+ and Cu_{pl}^{2+}. Note a large band gap of 1.6 eV and a valence band consisting of 36 O states coming from the p bands of the six O atoms. Below, and separated from the valence band, the ten localized Cu_{ch} states occur. These results are in agreement with the accepted charge balance model. However, this configuration is unfavorable by 3.9 eV and Fig. 1b shows the density of states for the ground state configuration of Cu_{ch}^{3+} and C_{pl}^{2+}. It is also an insulator, albeit with a smaller gap of 0.3 eV. This is achieved because the two Cu_{ch} d_{3z^2-1} orbitals which are treated with the LSD remain occupied but are hybridized into the top of the valence band; i.e., the number of valence states and the number of valence electrons have both increased by the same amount leaving the system in the insulating state. The calculations therefore show that Cu_{ch} d electrons contribute to the valence band.

For $YBa_2Cu_3O_{6.5}$ the ground state is metallic and nonmagnetic with a configuration of Cu_{ch}^{3+} and Cu_{pl}^{3+} (Table II

TABLE II. Energy differences with respect to the lowest total energy as calculated for a variety of Cu configurations (conf.) listed in Table I. Cu_{pl} and Cu_{ch} refer to planar and chain Cu, respectively. The energy differences are expressed in eV per CuO_2 layer.

Conf.						
Cu_{pl}	Cu_{ch}	$YBa_2Cu_3O_6$	Gap (eV)	$YBa_2Cu_3O_{6.5}$	Gap (eV)	$YBa_2Cu_3O_7$
d^9	d^{9*}	1.2	0.66	1.9	0.72	1.5
d^9	d^{8*}	0.0	0.30	1.0	0.56	1.0
d^9	d^{10}	3.9	1.29			2.1
d^9	d^9	4.35				2.2
d^9	d^8	4.2				1.95
d^8	d^{9*}	1.7		1.1		0.0
d^8	d^{8*}	0.55		0.0		0.07
d^8	d^{10}	4.5				0.6
d^8	d^9	4.7				0.6
d^8	d^8	4.6				0.8

YBa2Cu3O6
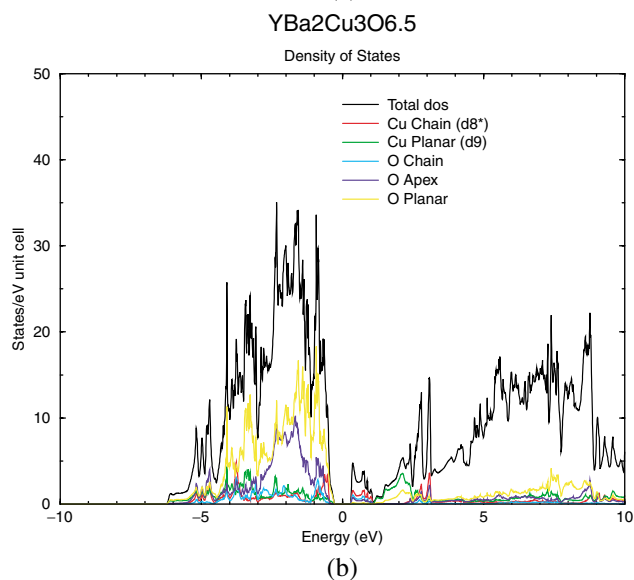
Density of States

(a)
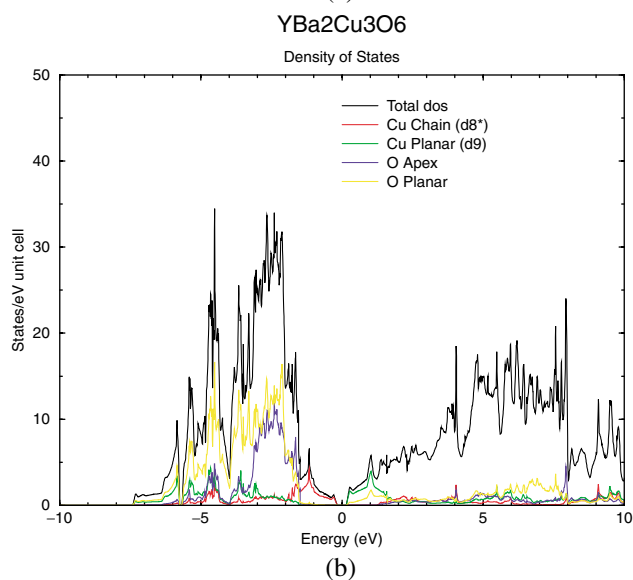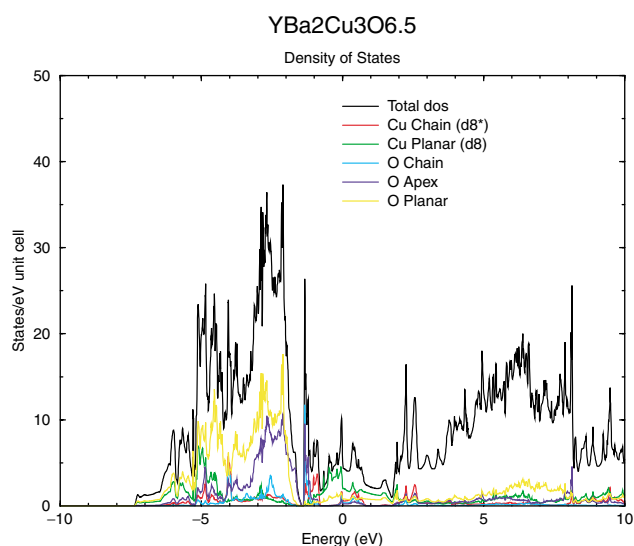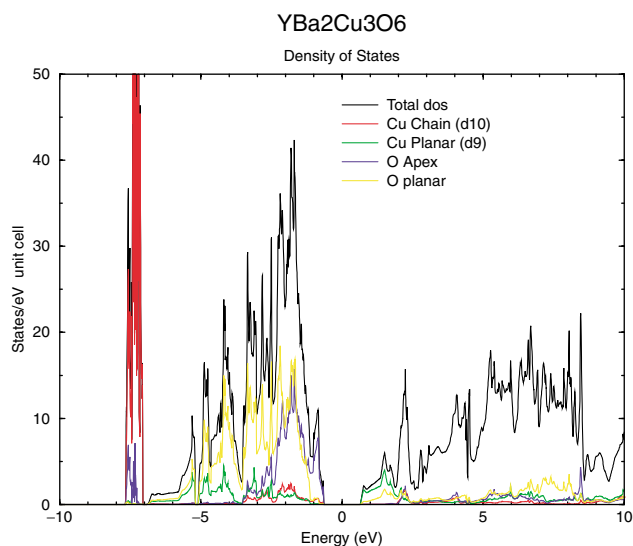
YBa2Cu3O6

Density of States

(b)

FIG. 1 (color).   The density of states of $YBa_2Cu_3O_6$ with Cu_{ch} configurations of d^{10} (a) and d^{8*} (b) and with Cu_{pl} kept in the d^9 configuration. The Fermi level is at zero energy.

YBa2Cu3O6.5

Density of States

(a)

YBa2Cu3O6.5

Density of States

(b)

FIG. 2 (color).   The density of states of $YBa_2Cu_3O_{6.5}$ with Cu_{ch} and Cu_{pl} configurations of d^{8*} and d^8, respectively (a) and d^{8*} and d^9, respectively (b). The Fermi level is at zero energy.

and Fig. 2a). However, the configuration Cu_{ch}^{3+} and Cu_{pl}^{2+} is only 1 eV away in energy, and in this configuration the insulating state of the O_6 compound is maintained, as seen in Fig. 2b. This is accomplished by one of the two Cu_{ch} states becoming unoccupied. Therefore, plausibly, the configuration Cu_{ch}^{3+} and Cu_{pl}^{2+} can be expected to give rise to insulating behavior for all O concentrations between O_6 and $O_{6.5}$. By adding O, in going from O_6 to $O_{6.5}$, the Cu_{pl} d bands move up in energy (compare Figs. 1b and 2b) and consequently it becomes favorable to delocalize one of the nine localized Cu_{pl} electrons. Comparison of Figs. 2a and 2b illustrates how the number of planar Cu d states increases in the valence band as the localized d shell changes from d^9 to d^{8*}.

The Cu_{pl}^{3+} remains the state with the lowest energy in $YBa_2Cu_3O_7$, however, with a near degeneracy between

divalent and trivalent Cu_{ch} (Table II). Also the monovalent Cu_{ch} configuration is now closer in energy, suggesting that valence fluctuations on Cu_{ch} are more pronounced in the O_7 compound. The influence of the structural aspects on the valency of Cu_{ch} in $YBa_2Cu_3O_7$ is illustrated in Table III, which suggests a strong coupling between the Cu_{ch} valence fluctuations and the O4 position. The Cu_{ch}–O4 (i.e., the apex O) bond length is small at 1.85 Å for $YBa_2Cu_3O_7$ but still slightly bigger than in $YBa_2Cu_3O_{6.5}$ at 1.824 and 1.813 Å in $YBa_2Cu_3O_6$. At these bond lengths the Cu_{ch} is trivalent in the O_6 and $O_{6.5}$ compounds but becomes divalent in the O_7 compound. However, a slight reduction in bond length of less than 2% changes the valency to trivalent. The reduced bond length increases the Cu_{ch}-O4 interaction in such a manner

TABLE III.   Bond lengths of apex O4 to Cu_{ch} and Cu_{pl} together with the valencies of the Cu_{ch} and Cu_{pl} for $YBa_2Cu_3O_6$, $YBa_2Cu_3O_{6.5}$, and $YBa_2Cu_3O_7$ in Å units. The only structural quantity changed in these calculations is the internal parameter determining the position of the apex O4 in the unit cell. The Δ refers to the energy difference between divalent and trivalent Cu_{ch}. Note that the Cu_{ch} becomes trivalent for a 2% reduction in the $O4-Cu_{ch}$ (Å) bond length. Expt. refers to the use of the experimental bond lengths and $O_{6.5}$ geom. means calculating the O_7 compound on the lattice of the $O_{6.5}$ compound.

	Bond length $O4-Cu_{ch}$ (Å)	Valency Cu_{ch}	Bond length $O4-Cu_{pl}$ (Å)	Valency Cu_{pl}	
$YBa_2Cu_3O_6$	1.813	3+	2.450	2+	expt.
$YBa_2Cu_3O_{6.5}$	1.824	3+	2.389	3+	expt.
$YBa_2Cu_3O_7$					
$\Delta = -0.07$ eV	1.850	2+	2.304	3+	expt.
$\Delta = -0.02$ eV	1.831	2+	2.323	3+	-1% in bond length
$\Delta = 0.05$ eV	1.812	3+	2.342	3+	-2% in bond length
$\Delta = 0.5$ eV	1.704	3+	2.450	3+	-8% in bond length
	1.824	3+	2.389	3+	$O_{6.5}$ geom.

that it becomes more favorable for the Cu_{ch} d_{3z^2-1} electron to become bandlike and hence a change to trivalency occurs. This change of valency is purely structural since increasing the O content from $O_{6.5}$ to O_7, while keeping the structural parameters of $O_{6.5}$, does not change the Cu_{ch} valency. The resulting band structure of $YBa_2Cu_3O_7$, with Cu_{pl}^{3+} and Cu_{ch}^{3+}, is very similar to that of the LSD approximation in the vicinity of the Fermi energy.

In conclusion, we have demonstrated that the SIC-LSD formalism allows for a consistent and unified description of the YBCO compounds going from O_6 to O_7. In these systems the change of the electronic properties from insulating and antiferromagnetic to metallic is described by the change of valency of Cu_{pl}^{2+} to Cu_{pl}^{3+}. The addition of O in YBCO introduces upward chemical shifts of the Cu $d_{x^2-y^2}-O2\ p_x-O3\ p_y$ bands, resulting in the transfer of the localized majority spin Cu $d_{x^2-y^2}-O2\ p_x-O3\ p_y$ state to the valence band, together with the disappearance of divalent and magnetic Cu and the appearance of trivalent and nonmagnetic Cu in the CuO_2 plane. In other words, the Cu $d_{x^2-y^2}-O2\ p_x-O3\ p_y$ bands in both spin channels become part of the valence band. Other noteworthy points are (1) the density of states of the antiferromagnetic and insulating state of $YBa_2Cu_3O_6$ reveals more Cu_{ch} valence states than expected from the standard ionic picture, (2) the ground states of $YBa_2Cu_3O_{6.5}$ and $YBa_2Cu_3O_7$ are calculated to be metallic, while $YBa_2Cu_3O_6$ is correctly described as antiferromagnetic and insulating, (3) no valency change needs to be invoked to obtain an antiferromagnetic and insulating state of $YBa_2Cu_3O_{6.5}$, and, finally, (4) a strong coupling exists between Cu_{ch} valence fluctuations and the O4 vibrational mode in $YBa_2Cu_3O_7$.

[1] S.-C. Zhang, Science **275**, 1089 (1997).
[2] W. M. Temmerman, H. Winter, Z. Szotek, and G. Y. Guo, Physica (Amsterdam) **172B**, 279 (1991).
[3] H. Winter, Z. Szotek, and W. M. Temmerman, Z. Phys. B **79**, 241 (1990).
[4] J. P. Perdew and A. Zunger, Phys. Rev. B **23**, 5048 (1981).
[5] A. Svane, Phys. Rev. Lett. **68**, 1900 (1992); W. M. Temmerman, Z. Szotek, and H. Winter, Phys. Rev. B **47**, 11 533 (1993).
[6] H. Ding, A. F. Bellman, J. C. Campuzano, M. Randeria, M. R. Norman, T. Yokoya, T. Takahashi, H. Katayama-Yoshida, T. Mochiku, K. Kadowaki, G. Jennings, and G. P. Brivio, Phys. Rev. Lett. **76**, 1533 (1996).
[7] R. S. Markiewicz, J. Phys. Chem. Solids **58**, 1179 (1997); Z. Szotek, B. L. Gyorffy, W. M. Temmerman, and O. K. Andersen, Phys. Rev. B **58**, 522 (1998).
[8] A. Svane and O. Gunnarsson, Phys. Rev. Lett. **65**, 1148 (1990); Z. Szotek, W. M. Temmerman, and H. Winter, Phys. Rev. B **47**, 4029 (1993); M. Arai and T. Fujiwara, Phys. Rev. B **51**, 1477 (1995).
[9] P. Strange, A. Svane, W. M. Temmerman, Z. Szotek, and H. Winter, Nature (London) **399**, 756 (1999).
[10] W. M. Temmerman, A. Svane, Z. Szotek, and H. Winter, in *Electronic Density Functional Theory: Recent Progress and New Directions,* edited by J. F. Dobson, G. Vignale, and M. P. Das (Plenum, New York, 1998).
[11] O. K. Andersen and O. Jepsen, Phys. Rev. Lett. **53**, 2571 (1984); O. K. Andersen, A. V. Postnikov, and S. Y. Savrasov, Mater. Res. Soc. Symp. Proc. **253**, 37 (1992).
[12] J. S. Swinnea and H. Steinfink, J. Mater. Res. **2**, 424 (1987).
[13] J. D. Jorgensen, B. W. Veal, A. P. Paulikas, L. J. Nowicki, G. W. Crabtree, H. Claus, and W. K. Kwok, Phys. Rev. B **41**, 1863 (1990).
[14] A. W. Hewat, J. J. Capponi, C. Chaillout, M. Marezio, and E. A. Hewat, Solid State Commun. **64**, 301 (1987).
[15] W-H. Li, J. W. Lynn, and Z. Fisk, Phys. Rev. B **41**, 4098 (1990); S. Shamoto, M. Sato, J. M. Tranquada, B. J. Stern-lieb, and G. Shirane, Phys. Rev. B **48**, 13 817 (1993).